Glycobiology, 2018, vol. 28, no. 4, 214–222
doi: 10.1093/glycob/cwy005
Advance Access Publication Date: 13 January 2018
Original Article

OXFORD

Analytical Glycobiology

Isotopic labeling with cellular O-glycome reporter/amplification (ICORA) for comparative O-glycomics of cultured cells

Matthew R Kudelka[2,3], Alison V Nairn[4], Mohammed Y Sardar[2], Xiaodong Sun[2], Elliot L Chaikof[2], Tongzhong Ju[3,4], Kelley W Moremen[5], and Richard D Cummings[2,1]

[2]Department of Surgery, Beth Israel Deaconess Medical Center, Harvard Medical School, Boston, MA, USA, [3]Department of Biochemistry, Emory University School of Medicine, Atlanta, GA, USA, [4]Office of Biotechnology Products, Center for Drug Evaluation and Research, U.S. Food and Drug Administration, Silver Spring, MD, USA, and [5]Complex Carbohydrate Research Center, University of Georgia, Athens, GA, USA

[1]To whom correspondence should be addressed: Tel: +1-617-735-4643; Fax: +1-617-735-4640; e-mail: rcummin1@bidmc.harvard.edu

Received 21 November 2017; Revised 11 January 2018; Editorial decision 11 January 2018; Accepted 24 January 2018

Abstract

Mucin-type O-glycans decorate >80% of secretory and cell surface proteins and contribute to health and disease. However, dynamic alterations in the O-glycome are poorly understood because current O-glycomic methodologies are not sufficiently sensitive nor quantitative. Here we describe a novel isotope labeling approach termed Isotope-Cellular O-glycome Reporter Amplification (ICORA) to amplify and analyze the O-glycome from cells. In this approach, cells are incubated with Ac_3GalNAc-Bn (Ac_3GalNAc-[$^1H_7$]Bn) or a heavy labeled Ac_3GalNAc-Bn^{D7} (Ac_3GalNAc-[$^2D_7$]Bn) O-glycan precursor (7 Da mass difference), which enters cells and upon de-esterification is modified by Golgi enzymes to generate Bn-O-glycans secreted into the culture media. After recovery, heavy and light Bn-O-glycans from two separate conditions are mixed, analyzed by MS, and statistically interrogated for changes in O-glycan abundance using a semi-automated approach. ICORA enables ~100–1000-fold enhanced sensitivity and increased throughput compared to traditional O-glycomics. We validated ICORA with model cell lines and used it to define alterations in the O-glycome in colorectal cancer. ICORA is a useful tool to explore the dynamic regulation of the O-glycome in health and disease.

Key words: colorectal cancer, glycomics, mucin-type O-glycans, O-glycans, stable isotope labeling

Introduction

Protein glycosylation is an abundant post-translational modification and involved in diverse processes ranging from cell signaling to tissue homeostasis (Apweiler et al. 1999; Ohtsubo and Marth 2006; Steentoft et al. 2013). Normal glycosylation is disturbed in many diseases, making glycans a powerful biomarker to follow disease course, predict treatment and understand pathology (Ohtsubo and Marth 2006). Ordinary sequencing of glycans requires chemical and/or enzymatic release followed by mass spectrometry (MS) (Cummings and Pierce 2014). Although this provides valuable qualitative information, glycan release requires relatively large sample sizes, limiting glycomics in many important settings, and cannot easily be done to study signaling/metabolic changes associated with altered glycosylation.

Stable isotope labeling is a powerful approach to quantify changes in glycan expression. As in proteomics, glycans can be

labeled after extraction with stable isotope tags, either by permethylation or reducing end tags, or prior to extraction by metabolic incorporation of heavy nitrogen (Gygi et al. 1999; Ong et al. 2002; Yuan et al. 2005; Alvarez-Manilla et al. 2007; Orlando et al. 2009). Since stable isotope labeling results in a mass shift, labeled and unlabeled samples can be mixed and analyzed by mass spectrometry to assess relative changes in glycan expression. While labeling at the reducing end results in fixed mass tags, permethylation or metabolic incorporation results in dynamic mass tags with mass shifts that depend on glycan size and composition, complicating analyses.

Mucin type O-glycans in O-GalNAc-linkage to Ser/Thr/Tyr residues decorate >80% of proteins that traverse the secretory apparatus and are altered in various human biological processes, such as leukocyte trafficking, and also in diseases, such as cancer and inflammatory bowel disease (IBD), but current strategies to assess these O-glycan structures and changes are limited (An et al. 2007; Fu et al. 2011; Furukawa et al. 2013; Ju et al. 2013, 2014; Steentoft et al. 2013; Kudelka et al. 2015, 2016b). Because there are no enzymes capable of releasing complex-type O-glycans from proteins or peptides, analysis requires inefficient chemical release methods that result in glycan degradation and poor signal-to-noise (Furukawa et al. 2013). Additionally, reduction of the reducing glycan to the alditol derivative during release prevents further labeling at the reducing end and in most cases reliance on dynamic mass tags for quantitative glycomics. To aid in O-glycan analysis, we recently developed a technology termed cellular O-glycome reporter/amplification (CORA) that bypasses glycan release and amplifies the O-glycome from cultured cells, resulting in 100–1000× increased sensitivity over traditional methods (Kudelka et al. 2016a). In CORA, a peracetylated chemical O-glycan precursor (Ac_3GalNAc-Bn) is added to cells, crosses the plasma membrane, is de-esterified, taken up into the Golgi apparatus, and modified by endogenous glycosyltransferases utilizing native sugar donors before being secreted for easy purification and MS analysis.

Here, we have modified CORA for quantitative glycomics by utilizing a stable isotope labeled Ac_3GalNAc-Bn precursor with a deuterated benzyl group that is 7 Da heavier than its protonated counterpart. These D_7 heavy labeled Bn^{D7}-O-glycans can be mixed with light Bn^{H7}-O-glycans generated from cells for sensitive and reproducible relative quantification within a 10-fold linear range. We term this technology isotopic labeling with cellular O-glycome reporter/amplification (ICORA). Using this approach, we evaluated alterations in the O-glycome in colorectal cancer and identified specific differences in O-glycan biosynthesis. ICORA combines the advantages of fixed mass stable isotope labeling with glycome amplification for sensitive, high-throughput, comparative/quantitative cellular O-glycomics.

Results

Overview of isotopic labeling with cellular O-glycome reporter/amplification (ICORA)

Although CORA is a powerful tool to assess qualitative changes in O-glycosylation, we sought to introduce a heavy isotope label into Bn-α-GalNAc $(Ac)_3$, which along with the unlabeled precursor can be used to assess quantitative changes in the glycome, similar to SILAC for proteomics (Ong et al. 2002). We envisioned that a cell line undergoing condition A can be incubated with the light, unlabeled Ac_3GalNAc-Bn^{H7} while the same cell line undergoing condition B can be incubated with the heavy, deuterium labeled Ac_3GalNAc-Bn^{D7} precursor (Figure 1). Media from the two conditions can then be mixed and Bn-O-glycans isolated and analyzed as with CORA. A relative change in abundance can be detected by assessing the ratio of the light Bn-O-glycans to the heavy Bn-O-glycans in biological replicate to statistically interrogate changes in glycosylation, both for individual glycans, such as those resulting from transcriptional induction/repression of specific glycosyltransferases, as well as overall changes in the O-glycome, for example resulting from global alterations in glycome synthesis. We term this approach Isotope-Cellular O-glycome Reporter/Amplification, or ICORA.

Generation of a heavy labeled Ac_3GalNAc-Bn^{D7} precursor

An isotopic label can be introduced into the aglycone (benzyl group) or glycone (*N*-acetylgalactosamine) of the peracetylated Bn-α-GalNAc precursor. Although stable isotope labels are thought to be biologically indistinguishable from their light isotope counterparts, we decided to modify the aglycone to minimize any potential disruption of glycan extension of the GalNAc. We wished to generate a heavy isotope label with a shift of at least 5 Da to avoid overlap

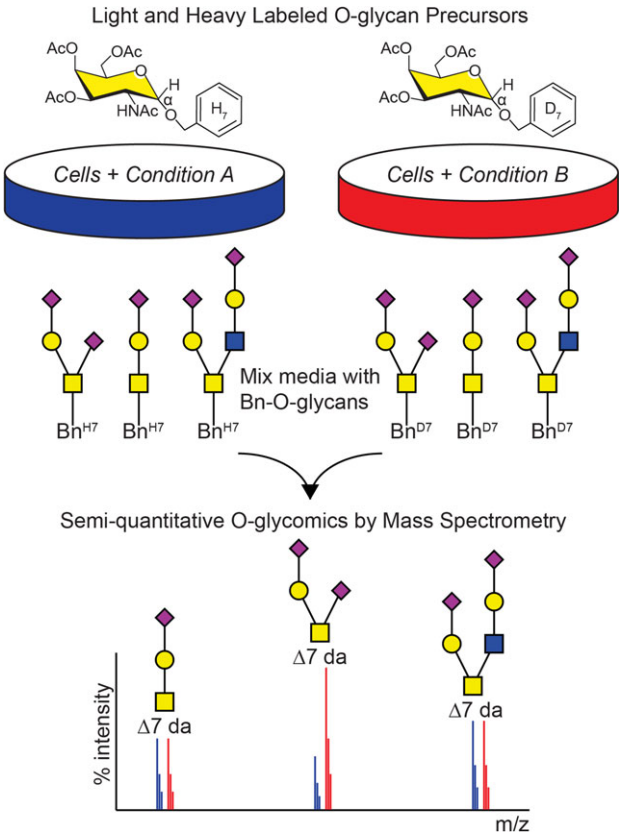

Fig. 1. Overview of isotopic labeling with cellular O-glycome reporter/amplification (ICORA). Cells undergoing condition A are incubated with Ac_3GalNAc-Bn^{H7} while cells undergoing condition B are incubated with Ac_3GalNAc-BnD_7. Ac_3GalNAc-Bn crosses the plasma membrane, is de-esterified in the cytosol, taken up into the Golgi apparatus, and modified by endogenous glycosyltransferases to produce light H_7 or heavy D_7 labeled Bn-O-glycans before being secreted into the media. Media from the two conditions is mixed together and heavy and light Bn-O-glycans are purified, permethylated, and analyzed by mass spectrometry. A 7 Da mass shift distinguishes the light and heavy O-glycans, enabling quantification of shifts in relative abundance and comparison of O-glycans in condition A versus condition B.

with peaks from the normal isotopic distribution of the light labeled counterpart. Incorporation of $^{13}C_6$ benzyl or D_7 benzyl into Ac_3GalNAc-Bn would both fulfill these criteria; however, D_7 benzyl alcohol is easier to synthesize or obtain than $^{13}C_6$ benzyl alcohol. Accordingly, we synthesized Ac_3GalNAc-Bn^{D7} from D_7 benzyl alcohol and $(Ac)_3$SPh-GalNAc-N_3, as outlined in Supplementary data, Figure S1, to form the heavy labeled Ac_3GalNAc-Bn^{D7} precursor. The Ac_3GalNAc-Bn^{D7} precursor has a predicted mass 7 Da heavier than the unlabeled Ac_3GalNAc-Bn^{H7} counterpart. We analyzed the heavy and light precursors by MALDI-MS and observed the expected masses of 460.3 *m/z* (Figure 2A) and 467.3 *m/z* (Figure 2B), respectively, corresponding to [M+Na]+ ions. Importantly, when we mixed these two compounds in a ratio of 1:1 and performed MALDI, we obtained a ratio of peak intensities of L:H of approximately 1:1, indicating that the deuterated precursor ionizes similarly to the protonated precursor (Figure 2C and D).

Ac_3GalNAc-Bn^{H7} and Ac_3GalNAc-Bn^{D7} are processed equivalently in cells

Before using heavy or light labeled Ac_3GalNAc-Bn precursors for comparative O-glycomics, we asked whether the two compounds are processed similarly in cells. We incubated HEK-293 cells with 50 µM of Ac_3GalNAc-Bn^{H7} or Ac_3GalNAc-Bn^{D7} in a 12-well dish for 3 days, and separately isolated the Bn^{H7}-O-glycans and Bn^{D7}-O-glycans from cell culture media as described, with an additional C18 purification step as detailed in the *Methods* section (Kudelka et al. 2016a). Bn-O-glycans were then permethylated and analyzed by MALDI-TOF-MS. Light (Figure 3A) and heavy-labeled Bn-O-glycans (Figure 3B) produced a similar pattern of core 1 and 2-based structures with 0–2 sialic acids, 0–1 fucose, and LacNAc extension on the core 2 branch. To further compare relative abundances, we overlaid heavy and light spectra and found that they were nearly identical (Figure 3C and D). Thus, Ac_3GalNAc-Bn^{H7} and Ac_3GalNAc-Bn^{D7} are processed similarly in cells.

Comparative O-glycomics in adherent and suspension cells

We next asked whether we could mix Bn^{D7}-O-glycans and Bn^{H7}-O-glycans derived from the heavy and light precursors to provide a semi-quantitative analysis for comparative O-glycomics. We incubated adherent (HEK-293, Figure 4A) or suspension cells (MOLT-4, Figure 4B) with 50 µM Ac_3GalNAc-Bn^{H7} or Ac_3GalNAc-Bn^{D7} for 3 days, collected media, and mixed heavy or light-labeled media from the same cell line in a 1:1 ratio before purification, permethylation, and MS analysis of Bn-O-glycans. We compared ratios of Bn^{H7}-O-glycans to Bn^{D7}-O-glycans for 13 glycans for HEK-293 cells and six glycans for MOLT-4 cells (Figure 4A and B). Across all glycans, the average L:H ratio was 1.21 ± 0.01 (mean ± SD) for HEK-293 cells and 1.32 ± 0.03 (mean ± SD) for MOLT-4 cells with a range of L:H ratios for individual glycans of 1.01–1.51 for HEK-293 cells and 0.95–1.98 for MOLT-4 cells. Most importantly, the ratios of L:H intensities were highly reproducible across independent experiments (Figure 4A and B), suggesting that deviations of L:H from 1:1 likely reflect slight differences in precursor concentrations of stock solutions prior to addition to cells. To account for this, the L:H ratios for treated cells could be normalized to the L:H of untreated cells during comparative O-glycomics. By analyzing individual spectra, we saw a similar pattern with L:H close to 1:1 for both HEK-293 (Figure 4C) and MOLT-4 cells (Figure 4D) with heavy labeled peaks fully separated from light Bn-O-glycan peaks along with their

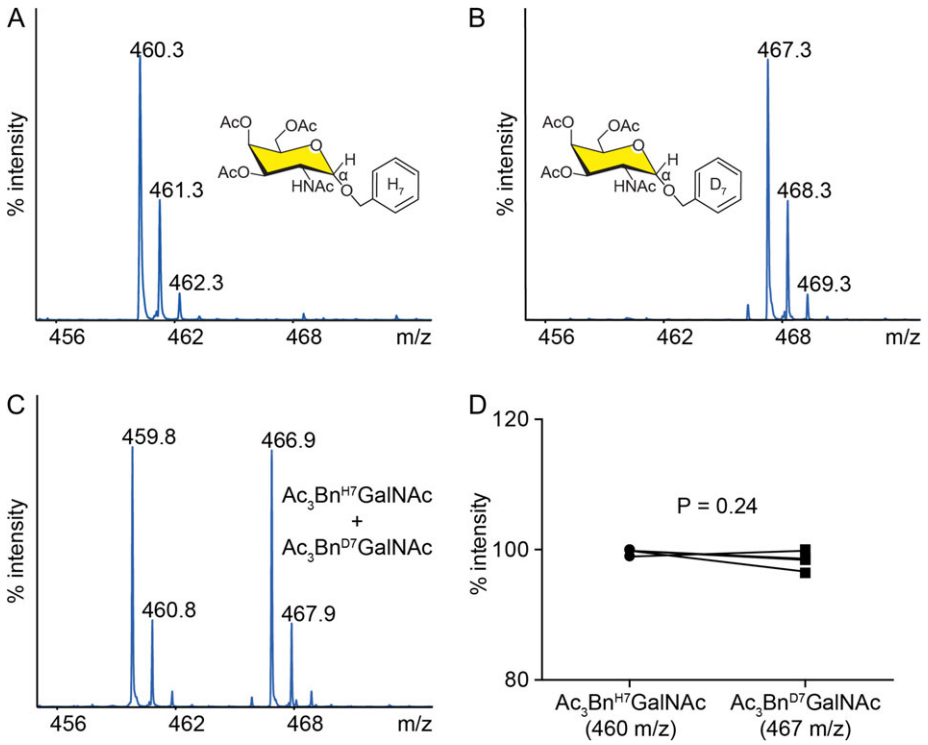

Fig. 2. Validation of heavy isotope labeled Ac_3GalNAc-Bn O-glycan precursor. MALDI-TOF-MS analysis of unlabeled Ac_3GalNAc-Bn^{H7} (**A**) and heavy labeled Ac_3GalNAc-Bn^{D7} (**B**) O-glycan precursors. (**C**) Representative spectra or (**D**) summary data ($n = 4$) of heavy and light labeled precursors mixed 1:1. Two-tailed *t*-test performed for **D**; **A**,**B** repeated two-independent times.

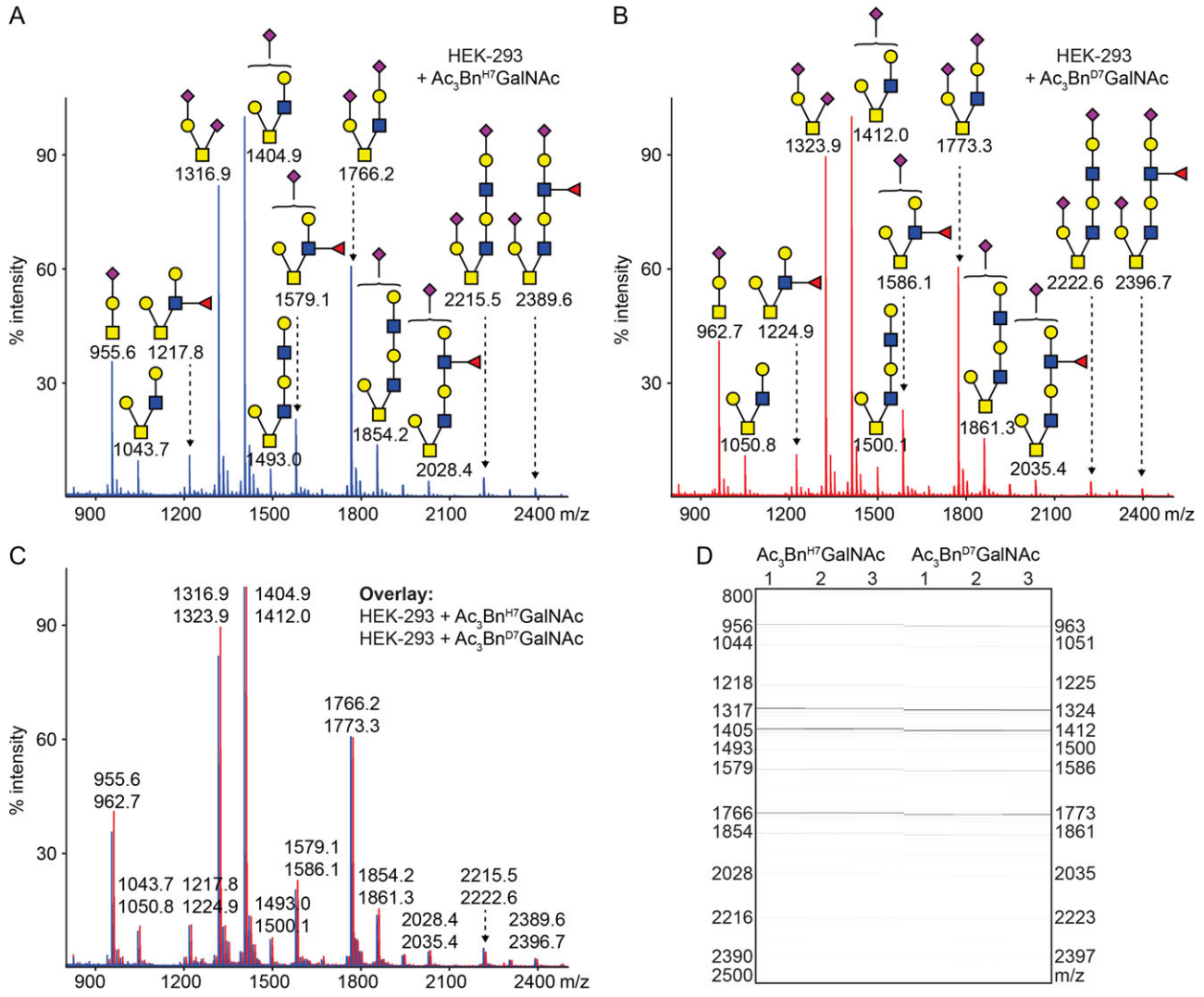

Fig. 3. Heavy and light labeled O-glycan precursors behave similarly in cells. MS analysis of permethylated Bn-O-glycans produced from HEK-293 cells incubated with 50 μM of $Ac_3GalNAc\text{-}Bn^{H7}$ (**A**,**C**,**D**) or $Ac_3GalNAc\text{-}Bn^{D7}$ (**B–D**). Individual spectra shown for **A**,**B** or overlaid in **C**. (**D**) MS intensities shown in gel view for light and heavy Bn-O-glycans ($n = 3$). Structures were inferred from MS compositions and knowledge of biosynthetic machinery.

respective isotopic distributions. Thus, ICORA is an advantageous technology for comparative O-glycomics.

Semi-automated detection of O-glycans with ICORA

A major goal of computational glycomics is automated peak assignment of MS spectra. A variety of tools have been developed for *N*-glycans with less success for O-glycans (Goldberg et al. 2005, 2006; North et al. 2009). One of the major challenges for O-glycans is that signal-to-noise and peak abundances are poor. We partially addressed this with CORA by amplifying the glycome, introducing a unique Bn mass tag, and permitting a vehicle only negative control. However, low abundance peaks are sometimes still challenging to assign. ICORA addresses this limitation by introducing a heavy isotope label to more definitively identify O-glycans by a 7 Da mass shift. As outlined in Supplementary data, Figure S2, we performed all analyses in biological triplicate, spotted permethylated glycans from each biological replicate in technical triplicate, and then performed MS. Mass lists were then automatically extracted, filtered based on a theoretical mass list of all possible monosaccharide combinations, evaluated for a 7 Da shift, and then manually assessed to convert the *m/z* corresponding to some combination of monosaccharides to a likely O-glycan structure. All steps except for the last step were fully automated, successfully annotating O-glycans from the MS spectra.

Sensitive detection of small changes in O-glycan abundance

One of the potential strengths of our approach is to detect small changes in the relative abundance of glycans within a complex repertoire. To test this, we incubated HEK-293 cells with 50 μM of $Ac_3GalNAc\text{-}Bn^{H7}$ or $Ac_3GalNAc\text{-}Bn^{D7}$ for 3 days and mixed media from the two conditions in ratios of 1:9, 1:3, 1:1, 3:1 and 9:1 (Figure 5). We normalized the ratios of L:H for all mixtures to the 1:1 mixture and compared the theoretical to experimental L:H intensities across nine major glycans. We only evaluated nine glycans here instead of the 16 described previously because minor peaks of the Bn^{D7} and Bn^{H7} tagged glycans were undetectable for the 1:9 and 9:1 mixtures for 7 of the prior 16 glycans, reflecting

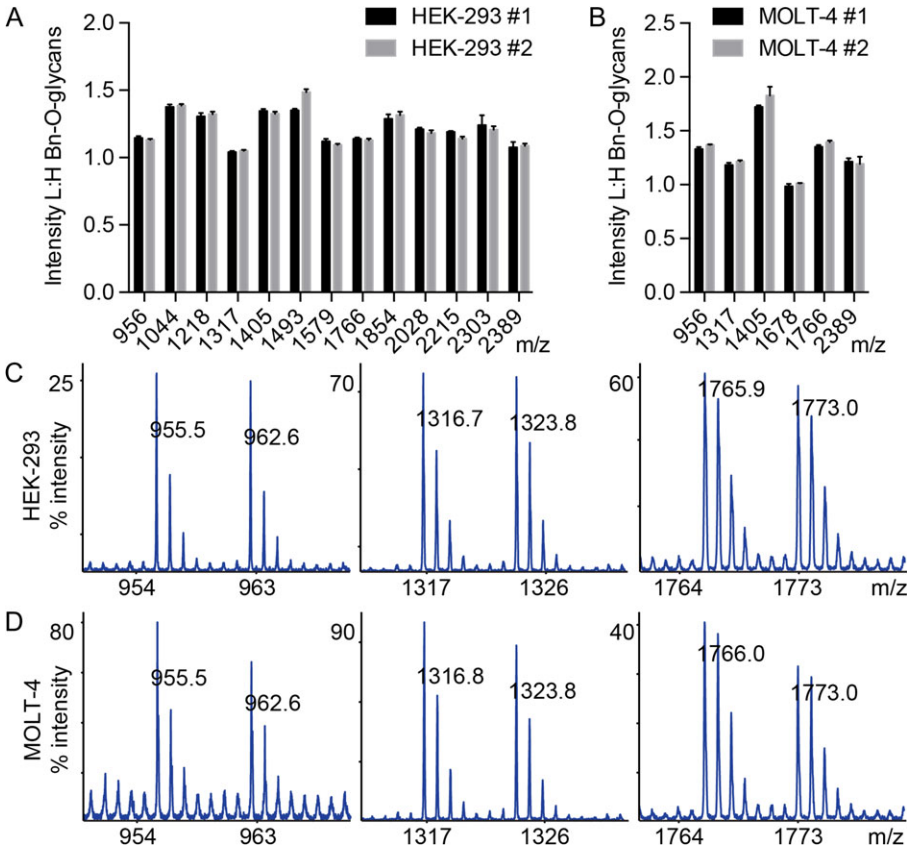

Fig. 4. Mixing of heavy and light labeled Bn-O-glycans from model cell lines. 50 μM $Ac_3GalNAc\text{-}Bn^{H7}$ and $Ac_3GalNAc\text{-}Bn^{D7}$ were respectively added to HEK-293 (**A**,**C**) and MOLT-4 (**B**,**D**) cells and mixed 1:1 prior to permethylation and MALDI-TOF-MS analysis. (**A**,**B**) L:H ratios were calculated for major glycans from two separate experiments ($n = 3$). Representative spectra are shown for monosialyl core 1 (956 *m/z*), disialyl core 1 (1317 *m/z*), and disialyl core 2 (1766 *m/z*) for HEK-293 (**C**) and MOLT-4 (**D**) cells. The most abundant glycan over the complete *m/z* range (not depicted here) was set to 100% intensity (**C**,**D**). Masses correspond to compositions shown in Figure 3.

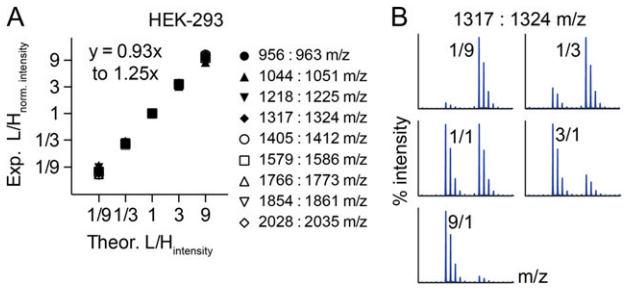

Fig. 5. ICORA detects changes in the relative abundance of O-glycans. Heavy and light 50 μM $Ac_3GalNAc\text{-}Bn$ O-glycan precursors were separately incubated with HEK-293 cells. Media from the cells were mixed in 1:9, 1:3, 1:1, 3:1 and 9:1 ratios. L:H ratios were normalized to L:H of 1:1 mixing and plotted as summary data ($n = 3$) (**A**) or shown as representative individual spectra for disialyl core 1 (**B**).

their reduced abundance in the HEK-293 O-glycome. We fitted a line comparing experimental (y) to theoretical (x) L:H intensities and found that these values highly correlated, with a slope ranging from $y = 0.93x$ to $y = 1.25x$ (Figure 5A and Supplementary data, Figure S2). In addition to evaluating normalized data from three biological replicates (Figure 5A, Supplementary data, Figure S2), we also evaluated individual spectra and saw a clear shift in Bn^{H7}- to Bn^{D7}-O-glycan abundances for L:H of 1:9, 1:3, 1:1, 3:1 and 9:1 (Figure 5B). Thus, ICORA can sensitively detect changes in O-glycans by isotopic labeling and mixing of Bn-O-glycans.

Altered O-glycosylation in colorectal cancer

O-glycans play diverse roles in tumor biology, however, the precise changes associated with tumor metastasis are poorly understood due to a lack of sensitive, quantitative technologies for O-glycomics (Kudelka et al. 2015). To address this, we applied ICORA to model colorectal cancer cell lines (Figure 6 and Supplementary data, Figure S4). SW480 and SW620 cells are derived from primary and metastatic colorectal cancer lesions from a single individual and retain some primary/metastatic features (Hewitt et al. 2000). We performed ICORA on SW480 and SW620 cells in biological triplicate, normalizing SW480:SW620 L:H ratios to SW480:SW480 L:H ratios (Figure 6A and Supplementary data, Figure S4). In total, we obtained 18 glycans for comparison, consisting of Core 1 and 2-based O-glycan structures and diverse terminal epitopes, including possible GalNAc, GlcNAc, α-Gal, blood group A, blood group B, polyLacNAc (-3Galβ1–4GlcNAcβ1-)$_n$, unmodified termini, sialylated termini, highly fucosylated structures, and LDNF (GalNAcβ1-4 [Fucα1-3]GlcNAcβ1-R). Although SW480/620 cells are classified as blood group A cells, trace levels of B-blood group have been previously demonstrated (Dahiya et al. 1989). Since α-Gal is an unusual structure in human cells, especially those containing blood group B, we performed MALDI-MS/MS on glycan 1421 *m/z* in SW480 cells.

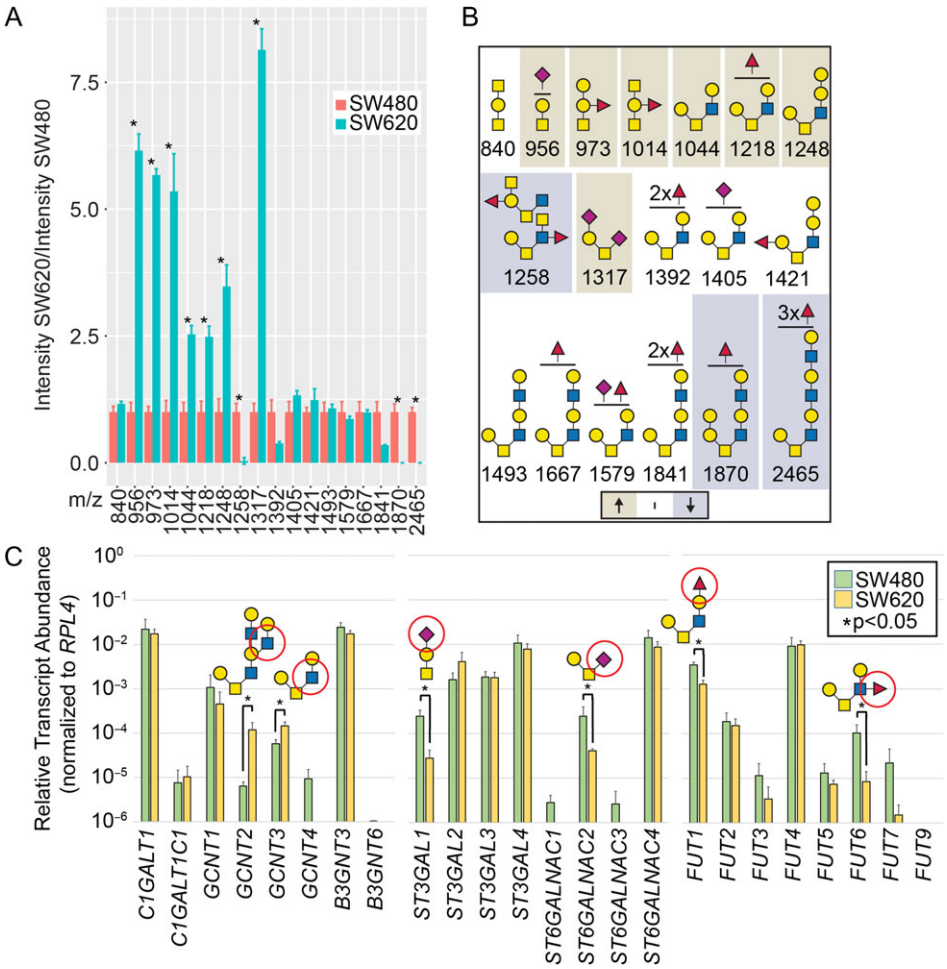

Fig. 6. O-glycomics and qRT-PCR of colorectal cancer cells. (**A**) ICORA was used to evaluate SW480 versus SW620 colorectal cancer cells; L:H ratios of SW480: SW620 were normalized to L:H of SW480:SW480 cells ($n = 3$; $^*P \leq 0.05$ from two-way ANOVA with Tukey's post hoc test for multiple comparison's). (**B**) Glycan structures shown from **A**; beige are statistically increased and gray decreased as defined in **A** for SW620 v. SW480 cells; structures are inferred from glycan composition, biosynthetic pathways, and partially from MS/MS data to be presented in a separate manuscript. (**C**) qRT-PCR of O-glycogenes from SW480 and SW620 cells. Data are plotted on a $\log_{10}$ scale and error bars represent SD ($n = 4$). Select synthetic pathways circled in red ($n = 4$; $^*P \leq 0.05$ from Mann–Whitney *U* Test).

Although we did not obtain linkage information and 1421 *m/z* was a relatively minor peak introducing some uncertainty in the MS/MS analysis, we found multiple fragments consistent with unfucosylated terminal Gal-Gal in a structure likely corresponding to Fucα1-2Galβ1-3[Galα1-3Galβ1-4GlcNAcβ1–6]GalNAcα1-Bn (Supplementary data, Figure S5, Table S1).

After assessing the repertoire of O-glycans in SW480 and SW620 cells, we evaluated changes in glycosylation. Of the 18 glycans analyzed, seven increased in SW620s (*m/z*: 956, 973, 1014, 1044, 1218, 1248, 1317), three decreased (*m/z*: 1258, 1870, 2465), and eight were unchanged (*m/z*: 840, 1392, 1405, 1421, 1493, 1667, 1579, 1841) (Figure 6A and B). Compared to SW480 cells, SW620 cells exhibited a reduction in larger glycans and a corresponding increase in smaller O-glycans. Reduced glycans were core 2-based, fucosylated (1–3 fucose), but not sialylated. In contrast, increased glycans were core 1 or core 2-based and contained unmodified, sialylated (1–2 Sia), and fucosylated (1 fucose) termini. The compositions of the increased glycans were consistent with blood group A containing structures, which were not present in the unchanged or reduced group, while compositions consistent with blood group B structures were present in all groups, and LDNF, which was only observed on one structure, was reduced in SW620s. Collectively these data provide a mixed picture in which SW620 cells exhibit reduced glycan size but increased complexity of glycan termini compared to SW480 cells.

To explore the transcriptional basis for altered O-glycosylation, we performed qRT-PCR transcript analysis of O-glycogenes predicted to be important in regulating the types of O-glycans found in the above analyses, including *C1GalT1 (T-synthase)*, *C1GalT1C1 (Cosmc)*, *GCNT1–4*, *B3GnT3* and *6*, *ST3Gal1*, *ST3Gal2*, *ST3Gal3*, *ST3Gal4*, *ST6GalNAc1*, *ST6GalNAc2*, *ST6GalNAc3*, *ST6GalNAc4*, and *Fut1*, *Fut2*, *Fut3*, *Fut4*, *Fut5*, *Fut6*, *Fut7* and *Fut9* (Figure 6C). Compared to SW480 cells, SW620 cells exhibited a change in 6 of the 24 transcripts with an increase in *GCNT2* and *GCNT3* and a reduction in *ST3Gal1*, *ST6GalNAc2*, *Fut1* and *Fut6*.

GCNT2 produces I antigen, which was not observed in SW480/620 O-glycans. In contrast, the other altered transcripts encode enzymes that synthesize structures present on SW480/620 O-glycans. *GCNT3* produces Core 2, *ST3Gal1* and *ST6GalNAc2* produce sialyl and disialyl Core 1 (with addition of NeuAc on Gal and GalNAc, respectively),

and *Fut1* and *Fut6* fucosylate galactose (to form Blood group-H) and GlcNAc, respectively. Based on transcriptional changes alone, these would predict increased Core 2-based structure (ST3Gal1 competes with GCNT3), reduced monosialyl and disialyl Core 1, and reduced fucosylation. Transcripts and structures correlate for fucosylation; however, other alterations in the transcriptome do not fully predict changes in the glycome. Therefore, additional factors such as Golgi architecture, glycoprotein flux, and transcript stability/turnover probably also help to regulate the colorectal O-glycome. Thus, these results demonstrate that O-glycosylation in SW480 versus SW620 colorectal cancer cells differ in specific O-glycan structures and gene expression.

Discussion

Here, we provide a novel stable isotope-based metabolic strategy to explore comparative O-glycomics through chemical synthesis using a stable isotope labeled O-glycome precursor, $Ac_3GalNAc\text{-}Bn^{D7}$. Addition of a light and heavy precursor to cells followed by mixing and analysis of differentially labeled Bn-O-glycans allows quantitative comparisons of O-glycan abundance in the same spectrum. Although metabolic stable isotope labeling has been previously applied to glycomics (Orlando et al. 2009), ICORA is the first to combine glycome amplification with stable isotope labeling for comparative O-glycomics. Thus, we can now study metabolic, signaling, and transcriptionally dependent changes in O-glycosylation in living cells. This approach opens the way to identifying specific inhibitors and signaling regulators of O-glycosylation.

The importance of these studies arises from the growing evidence that O-glycans are an abundant post-translational modification and contribute to regulating many biological processes (Steentoft et al. 2013; Kudelka et al. 2015). However, the structures normally present in cells and how they change in disease are not well understood. Part of the problem in studying O-glycans in cultured cells is that O-glycans are often relatively low in abundance, small in size, and a single plate of cultured cells does not provide enough material for robust glycan analysis and sequencing. Thus, ICORA provides many advantages. In addition to analyzing different cell populations or cells undergoing different treatment conditions, ICORA can also be used for semi-automated glycomics. The signal-to-noise and mass accuracy of MALDI-MS for O-glycans usually necessitates manual interrogation. However, we found that by analyzing cells incubated with a light and heavy O-glycan precursor that we could extract mass lists and filter those based on monosaccharide compositions and a 7 Da mass shift. Together these two criteria were sufficient for automated peak extraction and assignment.

Using this approach, we were able to identify LDNF as an epitope on O-glycans in colorectal cancer cells. This structure is abundant on parasitic glycans, but infrequent in mammals (Prasanphanich et al. 2014). A recent report observed LDNF in gastric tissues (Ikehara et al. 2006; Jin et al. 2017), which is consistent with our results and suggests that LDN and its fucosylated derivative LDNF may be a common but unappreciated feature of the human GI tract. Given that LDN-type glycans are immunosuppressive on parasites and glycodelin, it is tempting to speculate that they may contribute to the tolerogenic environment of the human gut (Kawar et al. 2005).

Through mixing experiments we clearly showed that ICORA is able to reproducibly detect small changes <10-fold in glycan abundance. We applied this to evaluate altered O-glycosylation in two colorectal cancer cell lines derived from the same individual and found that SW620 cells had reduced glycan length and increased epitope diversity compared to SW480 cells. Except for fucosylation, these changes were not correlated with changes in gene transcript abundances, highlighting the complexity of glycome regulation (Cummings and Pierce 2014). Thus, ICORA and other high-throughput glycomics and glycoproteomics technologies will be critical in understanding the biological roles of glycans in different cells and tissue and offer significant advantages over transcriptomics, which do not fully predict the glycome. Importantly, some of our findings compared well with prior studies, including an increase in sialyl-T and Core 2-sLe structures as well as a reduction in ST6GalNAc2, changes shown to promote invasion/metastasis (Holst et al. 2015; Jia et al. 2017). Given the widespread impact of other quantitative -omics, this new approach combining glycome amplification and metabolic stable isotope labeling in ICORA will provide a much needed tool for dissecting the cellular O-glycome.

This approach has some limitations, including the need to use living cells for metabolic labeling, the need of cells to synthesize enough material in secretions for identification, and the potential for cells to secrete enzymes that may alter or destroy glycans once secreted. In regard to the latter, we showed previously that secreted Bn-O-glycans are stable in culture media (Kudelka et al. 2016a), indicating that there is little if any degradation of glycans upon secretion. Notably, although we analyzed secreted Bn-O-glycans from media, we previously showed that these structures mirror those obtained by traditional analyses of whole cell lysates, including cell surface and intracellular structures. This follows from the fact that our O-glycan precursors traverse the same pathways as cell surface and secreted glycoproteins. Although ICORA is unique in providing a 7 Da mass shift, it does not eliminate many limitations of glycan structural analysis by mass spectrometry such as MS/MS of low abundance species or mass accuracy of MALDI versus electrospray ionization. Thus, non-MS-based approaches are still important for structural confirmation of biologically significant glycans. Finally, the precise quantification of secreted Bn-O-glycan, which relies on weak absorbance in the UV range, is difficult and we are developing MS standards to aid in the quantification in the future.

The information that can be obtained by the ICORA method has important implications. Studies of living cells in culture, and perhaps in organoids, using ICORA could provide insights into changes in O-glycosylation associated with cell growth, cell adhesion, matrix interactions, growth factors and other biological signaling pathways. As we described previously, as few as 10^4 cells may be used in this approach, thus allowing semi-quantitative and qualitative studies to be performed that have not been approachable by conventional methods. Also, the isolated and differently labeled Bn-O-glycans can be useful standards and reagents for other studies, since it is possible to define a standard isotope-labeled set of Bn-O-glycans that can be stored indefinitely.

Materials and methods

Cell culture

HEK-293 cells were a kind gift from Dr. Henrik Clausen (University of Copenhagen). MOLT-4, SW480, SW620 cells were purchased from ATCC. All cells were cultured in 10% fetal bovine serum and 2% penicillin-streptomycin. HEK-293, MOLT-4, and SW480/SW620 were cultured in DMEM (Corning), RPMI (Corning), and L-15 (Corning), respectively. All were grown on polystyrene except MOLT-4 cells that were grown in suspension. HEK-293, SW480 and SW620 cells were seeded at 10^5 cells/mL in 1 mL of media in a 12-well dish (Figures 3, 4, 6) or in 5 mL of media in a T25 flask (Figure 5). Compound was added the next day in 2 mL (Figures 3,

4, 6) or 5 mL (Figure 5) of fresh media. MOLT-4 cells were seeded at 5×10^5 cell/mL in 1 mL of media in a 12-well dish (Figure 4) and compound was added the next day in an additional 1 mL of fresh media to a final volume of 2 mL. All cells were then incubated with compound for 3 days prior to collection, purification, permethylation and MS analysis.

Compounds

GalNAcαBn was purchased from Sigma and peracetylated as described (Kudelka et al. 2016a) to generate Ac_3GalNAc-Bn. Ac_3GalNAc-Bn^{D7} was synthesized from Bn^{D7}OH (Supplementary data, Figure S1). Both were suspended at 50 mM concentration in DMSO and stored at –20°C until use. Stock solutions were diluted in cell culture media to a final concentration of 50 μM to incubate with cells.

Glycan purification

Media was collected from cells incubated with 50 μM Ac_3GalNAc-Bn or Ac_3GalNAc-Bn^{D7} for 3 days and Bn-O-glycans or Bn^{D7}-O-glycans were purified with a centrifugal filter using a 10 kDa high mass cut-off (Amicon) followed by reverse phase C18 (Waters) chromatography as described (Kudelka et al. 2016a). Bn-O-glycans or Bn^{D7}-O-glycans were either directly purified from media or mixed in different ratios prior to purification. In Figure 4, all of the 2 mL of media collected from cells incubated with Ac_3GalNAc-Bn^{H7} or Ac_3GalNAc-Bn^{D7} was mixed together at a 1:1 ratio prior to purification. In Figure 5, 5 mL of media was collected from cells incubated with Bn^{H7}-O-glycans or Bn^{D7}-O-glycans and mixed together at a ratio of 1:9, 1:3, 1:1, 3:1 and 9:1 to a final volume of 1 mL. Three mL of PBS was then added to make a final volume of 4 mL prior to purification.

Glycan permethylation

After purification from media, Bn^{H7}-O-glycans and Bn^{D7}-O-glycans were permethylated by DMSO/NaOH slurry and methyl iodide as described (Kudelka et al. 2016a). Following chloroform extraction, permethylated Bn^{H7}-O-glycans and Bn^{D7}-O-glycans were further purified by reverse phase C_{18} chromatography, washed with an acetonitrile step-gradient, eluted by 50% acetonitrile, and dried by vacuum centrifugation (Jang-Lee et al. 2006). This substantially increased signal-to-noise compared to chloroform extraction alone.

Mass spectrometry

Permethylated Bn^{H7}-O-glycans and Bn^{D7}-O-glycans were suspended in 10 μL of methanol (Jang-Lee et al. 2006). 0.5 μL of glycan suspension was mixed 1:1 with 0.5 μL of 20 mg/mL 2,5-dihydrobenzoic acid (Sigma) in 80% methanol on a Bruker AnchorChip 384 BC target plate, air dried, and analyzed by MALDI-TOF mass spectrometry using Bruker Daltonics ultrafleXtreme TOF-TOF system and flexControl software. Five thousand shots were collected in reflectron positive (RP) mode in the 800–5000 *m/z* range for each spot after calibration by standard peptide mixture. Molecular ions correspond to $[M+Na]^+$.

Glycan analysis

Each experiment was performed in biological triplicate and each sample was spotted in technical triplicate to control for spot-to-spot variations. Mass peaks were identified and filtered in a semi-automated manner to identify those corresponding to O-glycans. Briefly, major mass peaks were identified from Bruker Daltonics flexAnalysis software using automatic peak picking (default settings) and compared against a glycan mass library generated from random combinations of monosaccharides. Bn-O-glycans generated from Ac_3GalNAc-Bn^{H7} versus Ac_3GalNAc-Bn^{D7} were identified and filtered by a 7 Da mass shift. Putative glycan peaks were manually verified and assigned putative structures based on biosynthetic knowledge. Peak abundances were extracted and statistically analyzed as described in *Statistics*. Representative spectra were generated from mMass 5.5.0 (Strohalm et al. 2008) and overlaid with glycan "cartoon" representations from Glycoworkbench (Ceroni et al. 2008; Damerell et al. 2012).

RNA isolation and qRT-PCR analysis

Colorectal cancer cells were harvested, flash-frozen in liquid nitrogen, and stored at –80°C until use. Total RNA isolation and cDNA synthesis on four biological replicates of each cell type was carried out as described previously (Nairn et al. 2007). The qRT-PCR reactions were performed in triplicate for each gene analyzed using primer pairs listed in Supplemental Table 2. Amplification conditions and data analysis was performed as described previously (Nairn et al. 2010). Briefly, Ct values for each gene were normalized with the control gene, *RPL4*, prior to calculation of relative transcript abundance followed by statistical analysis with the Mann–Whitney test using GraphPad InStat software.

Statistics

Ratios of abundances of Bn^{H7}-O-glycans to Bn^{D7}-O-glycans were averaged from technical triplicates to obtain a $mean_{spot}$ for each glycan. Statistics were performed on the $mean_{spot}$ from three biological replicates with GraphPad Prism or R program language as indicated in the figure legends.

Supplementary data

Supplementary data is available at *Glycobiology* online.

Funding

This work was supported by 3U01CA207821 to T.J., R01DK107405, U01GM116196 and RO1HL128237 to E.L.C., GM103490 to K.W.M., and U01CA168930 and P41GM103694 to R.D.C.

Acknowledgements

We thank Melina Galizzi for technical expertise, D. Smith for helpful discussions, and J. Heimburg-Molinaro for reviewing the manuscript.

Conflicts of interest statement

The authors declare no conflict of interest.

Abbreviations

Ac, acetyl; B3GnT3 and 6, β-1,3-*N*-acetylglucosaminyltransferase 3 and 6; Bn, benzyl; C1GalT1, core 1 β3-galactosyltransferase 1; C1GalT1C1, C1GalT1 specific chaperone 1; CORA, cellular O-glycome reporter/amplification; DMEM, Dulbecco's Modified Eagle Medium; DMSO, dimethyl sulfoxide; Fut1-7 and 9, fucosyltransferase 1–7 and 9; Gal, galactose; GalNAc,

N-acetylgalactosamine; GlcNAc, *N*-acetylglucosamine; GCNT1–4, glucosaminyl (*N*-acetyl) transferase 1–4; IBD, inflammatory bowel disease; ICORA, isotopic labeling with cellular O-glycome reporter/amplification; kDa, kilodalton; L-15, leibovitz; LacNAc, *N*-acetyllactosamine; LDNF, fucosylated LacdiNAc (GalNAcbβ1-4GlcNAc); MALDI, matrix-assisted laser desorption/ionization; MS, mass spectrometry; N_3, azide; NaOH, sodium hydroxide; PBS, phosphate buffered saline; RPMI, Roswell Park Memorial Institute; ST3Gal1-4, Gal-β-1,3-GalNAc-α-2,3-sialyltransferase 1-4; ST6GalNAc1-4, GalNAc α-2,6-sialyltransferase 1; Sia, sialic acid; SPh, thiophenol; TOF, time of flight.

References

Alvarez-Manilla G, Warren N.L., Abney T., Atwood J., Azadi P., York W.S., Pierce M., Orlando R. 2007. Tools for glycomics: Relative quantitation of glycans by isotopic permethylation using 13CH3I. *Glycobiology*. 17(7): 677–687.

An G, Wei B., Xia B., McDaniel J.M., Ju T., Cummings R.D., Braun J., Xia L. 2007. Increased susceptibility to colitis and colorectal tumors in mice lacking core 3-derived O-glycans. *J Exp Med*. 204(6):1417–1429.

Apweiler R, Hermjakob H, Sharon N. 1999. On the frequency of protein glycosylation, as deduced from analysis of the SWISS-PROT database. *Biochim Biophys Acta*. 1473(1):4–8.

Ceroni A, Maass K., Geyer H., Geyer R., Dell A., Haslam S.M. 2008. GlycoWorkbench: A tool for the computer-assisted annotation of mass spectra of glycans. *J Proteome Res*. 7(4):1650–1659.

Cummings RD, Pierce JM. 2014. The challenge and promise of glycomics. *Chem Biol*. 21(1):1–15.

Dahiya R, Itzkowitz S.H., Byrd J.C., Kim Y.S. 1989. ABH blood group antigen expression, synthesis, and degradation in human colonic adenocarcinoma cell lines. *Cancer Res*. 49(16):4550–4556.

Damerell D, Ceroni A., Maass K., Ranzinger R., Dell A., Haslam S.M. 2012. The GlycanBuilder and GlycoWorkbench glycoinformatics tools: Updates and new developments. *Biol Chem*. 393(11):1357–62.

Fu J, Wei B., Wen T., Johansson M.E., Liu X., Bradford E., Thomsson K.A., McGee S., Mansour L., Tong M. et al. 2011. Loss of intestinal core 1-derived O-glycans causes spontaneous colitis in mice. *J Clin Invest*. 121(4): 1657–1666.

Furukawa J.i, Fujitani N, Shinohara Y. 2013. Recent advances in cellular glycomic analyses. *Biomolecules*. 3(1):198–225.

Goldberg D, Sutton-Smith M., Paulson J., Dell A. 2005. Automatic annotation of matrix-assisted laser desorption/ionization N-glycan spectra. *Proteomics*. 5(4):865–875.

Goldberg D, Bern M., Li B., Lebrilla C.B. 2006. Automatic determination of O-glycan structure from fragmentation spectra. *J Proteome Res*. 5(6): 1429–1434.

Gygi SP, Rist B., Gerber S.A., Turecek F., Gelb M.H., Aebersold R. 1999. Quantitative analysis of complex protein mixtures using isotope-coded affinity tags. *Nat Biotechnol*. 17(10):994–999.

Hewitt RE, McMarlin A., Kleiner D., Wersto R., Martin P., Tsokos M., Stamp G.W., Stetler-Stevenson W.G. 2000. Validation of a model of colon cancer progression. *J Pathol*. 192(4):446–454.

Holst S, Wuhrer M, Rombouts Y. 2015. Glycosylation characteristics of colorectal cancer. *Adv Cancer Res*. 126:203–256.

Ikehara Y, Sato T., Niwa T., Nakamura S., Gotoh M., Ikehara S.K., Kiyohara K., Aoki C., Iwai T., Nakanishi H. et al. 2006. Apical Golgi localization of N,N'-diacetyllactosediamine synthase, beta4GalNAc-T3, is responsible for LacdiNAc expression on gastric mucosa. *Glycobiology*. 16(9):777–785.

Jang-lee J, North S.J., Sutton-Smith M., Goldberg D., Panico M., Morris H., Haslam S., Dell A. 2006. Glycomic profiling of cells and tissues by mass spectrometry: Fingerprinting and sequencing methodologies. *Methods Enzymol*. 415:59–86.

Jia L, Luo S., Ren X., Li Y., Hu J., Liu B., Zhao L., Shan Y., Zhou H. 2017. miR-182 and miR-135b mediate the tumorigenesis and invasiveness of colorectal cancer cells via targeting ST6GALNAC2 and PI3K/AKT pathway. *Dig Dis Sci*. 62(12):3447–3459.

Jin C, Kenny D.T., Skoog E.C., Padra M., Adamczyk B., Vitizeva V., Thorell A., Venkatakrishnan V., Lindén S.K., Karlsson N.G. 2017. Structural diversity of human gastric mucin glycans. *Mol Cell Proteomics*. 16(5):743–758.

Ju T, Wang Y., Aryal R.P., Lehoux S.D., Ding X., Kudelka M.R., Cutler C., Zeng J., Wang J., Sun X. et al. 2013. Tn and sialyl-Tn antigens, aberrant O-glycomics as human disease markers. *Proteomics Clin Appl*. 7(9–10): 618–31.

Ju T, Aryal R.P., Kudelka M.R., Wang Y., Cummings R.D. 2014. The Cosmc connection to the Tn antigen in cancer. *Cancer Biomark*. 14(1):63–81.

Kawar ZS, Haslam S.M., Morris H.R., Dell A., Cummings R.D. 2005. Novel poly-GalNAcbeta1-4GlcNAc (LacdiNAc) and fucosylated poly-LacdiNAc N-glycans from mammalian cells expressing beta1,4-N-acetylgalactosaminyltransferase and alpha1,3-fucosyltransferase. *J Biol Chem*. 280(13): 12810–12819.

Kudelka MR, Ju T., Heimburg-Molinaro J., Cummings R.D. 2015. Simple sugars to complex disease – mucin-type O-glycans in cancer. *Adv Cancer Res*. 126:53–135.

Kudelka MR, Antonopoulos A, Wang Y, Duong DM, Song X, Seyfried NT, Dell A, Haslam SM, Cummings RD, Ju T. 2016a. Cellular O-Glycome Reporter/Amplification to explore O-glycans of living cells. *Nat Methods*. 13(1):81–86.

Kudelka MR, Hinrichs B.H., Darby T., Moreno C.S., Nishio H., Cutler C.E., Wang J., Wu H., Zeng J., Wang Y. et al. 2016b. Cosmc is an X-linked inflammatory bowel disease risk gene that spatially regulates gut microbiota and contributes to sex-specific risk. *Proc Natl Acad Sci USA*. 113(51): 14787–14792.

Nairn AV, Kinoshita-Toyoda A., Toyoda H., Xie J., Harris K., Dalton S., Kulik M., Pierce J.M., Toida T., Moremen K.W. et al. 2007. Glycomics of proteoglycan biosynthesis in murine embryonic stem cell differentiation. *J Proteome Res*. 6(11):4374–4387.

Nairn AV, dela Rosa M, Moremen KW. 2010. Transcript analysis of stem cells. *Methods Enzymol*. 479:73–91.

North SJ, Hitchen P.G., Haslam S.M., Dell A. 2009. Mass spectrometry in the analysis of N-linked and O-linked glycans. *Curr Opin Struct Biol*. 19(5): 498–506.

Ohtsubo K, Marth JD. 2006. Glycosylation in cellular mechanisms of health and disease. *Cell*. 126(5):855–867.

Ong SE, Blagoev B., Kratchmarova I., Kristensen D.B., Steen H., Pandey A., Mann M. 2002. Stable isotope labeling by amino acids in cell culture, SILAC, as a simple and accurate approach to expression proteomics. *Mol Cell Proteomics*. 1(5):376–386.

Orlando R, Lim J.M., Atwood J.A., Angel P.M., Fang M., Aoki K., Alvarez-Manilla G., Moremen K.W., York W.S., Tiemeyer M. et al. 2009. IDAWG: Metabolic incorporation of stable isotope labels for quantitative glycomics of cultured cells. *J Proteome Res*. 8(8):3816–3823.

Prasanphanich NS, Luyai A.E., Song X., Heimburg-Molinaro J., Mandalasi M., Mickum M., Smith D.F., Nyame A.K., Cummings R.D. 2014. Immunization with recombinantly expressed glycan antigens from *Schistosoma mansoni* induces glycan-specific antibodies against the parasite. *Glycobiology*. 24(7):619–637.

Steentoft C, Vakhrushev S.Y., Joshi H.J., Kong Y., Vester-Christensen M.B., Schjoldager K.T., Lavrsen K., Dabelsteen S., Pedersen N.B., Marcos-Silva L. et al. 2013. Precision mapping of the human O-GalNAc glycoproteome through SimpleCell technology. *EMBO J*. 32(10):1478–1488.

Strohalm M, Hassman M., Kosata B., Kodícek M. 2008. mMass data miner: An open source alternative for mass spectrometric data analysis. *Rapid Commun Mass Spectrom*. 22(6):905–908.

Yuan J, Hashii N., Kawasaki N., Itoh S., Kawanishi T., Hayakawa T. 2005. Isotope tag method for quantitative analysis of carbohydrates by liquid chromatography-mass spectrometry. *J Chromatogr A*. 1067(1–2):145–152.